Heterogeneous Catalysis Hot Paper

DOI: 10.1002/anie.201305530

Atomically Thin Tin Dioxide Sheets for Efficient Catalytic Oxidation of Carbon Monoxide**

*Yongfu Sun, Fengcai Lei, Shan Gao, Bicai Pan, Jingfang Zhou, and Yi Xie**

The catalytic oxidation of CO using heterogeneous catalysts could provide one of the most promising ways for solving current urgent environmental pollution issues, because of its wide applications in automotive exhaust treatment, indoor air cleaning, and breathing apparatus.[1] Unfortunately, the low catalytic activities and poor stabilities of conventional catalysts seriously impede their practical applications. Although pioneering studies have demonstrated that some noble metals, such as Au and Pd, could effectively catalyze CO oxidation,[1b,2] their high cost, low abundance, and rapid deactivation at elevated temperatures hinder their applicability. Recently, noble-metal-free catalysts have sparked worldwide interest owing to their low cost, environmental friendliness, and outstanding thermal stability.[3] In this regard, tetragonal SnO_2, which has a rutile structure, would be a good choice. In addition to its low cost, minimal toxicity, abundance, and high melting point of 1630 °C,[4] the appeal of tetragonal SnO_2 also comes from its highly reactive lattice oxygen atoms and low calculated oxygen vacancy formation energy.[5] Despite these advantages, practical applications are still handicapped by its low efficiencies, especially at low temperatures;[6] this shortcoming is mainly due to the extremely low amount of active sites in previously prepared SnO_2 catalysts.

Since the first report of graphene in 2004, graphene and graphene-like atomically thin sheets have already resulted in a wealth of unprecedented functionalities.[7] As such, atomically thin sheets may represent ideal architectures for high-performance CO catalytic oxidation as they could offer an extremely large proportion of surface atoms, which could serve as catalytically active sites to efficiently adsorb CO and O_2 molecules.[8] Moreover, according to the widely accepted Mars van Krevelen mechanism for metal oxide catalyzed CO oxidation,[9] the adsorbed CO molecule can be oxidized by the neighboring low-coordinate lattice oxygen atom at the catalyst surface, thus simultaneously creating an oxygen vacancy; subsequently, the formed oxygen vacancy facilitates the dissociation of O_2 molecules into highly reactive oxygen atoms.[10] Furthermore, it is noticeable that the atomically thin sheets are usually accompanied by surface structural disorder,[7b,11] which always leads to a much higher density of states (DOS) at the edge of the valence band or conduction band and favors the fast CO diffusion along the 2D conducting channels and hence reacts with the dissociated O atoms.[7b,12] Thus, atomically thin sheets can fully optimize the catalytic oxidation of CO by fundamentally improving the elementary adsorption, dissociation, and diffusion steps.

The above factors mean that the controllable synthesis of atomically thin SnO_2 sheets is of great importance. To date, anisotropic layered bulk materials have been regarded as the most effective precursors for fabricating atomically thin sheets, owing to the weak van der Waals interaction between the layers.[7c,12] However, as for nonlayered compounds, especially tetragonal SnO_2 that has low anisotropy, the difficulty in the bond cleavage and the lack of intrinsic driving force for 2D anisotropic growth make the synthesis of their atomically thin sheets a great challenge.[13] Although the formation of ultrathin sheets of nonlayered CdSe and PbS could be achieved through surfactant-assisted solution-phase synthesis,[14] the requirement of removing organic surfactants would unfortunately make their fabrication into nanodevices difficult. Accordingly, it is highly desirable but challenging to develop a convenient pathway to synthesize clean atomically thin SnO_2 sheets.

Herein, we report the successful synthesis of clean five-atomic-layer-thick SnO_2 sheets by the chemical reaction between $SnCl_2{\cdot}2H_2O$ and ethylenediamine. The TEM images in Figure 1A,B and the SEM image in Figure S3A (see the Supporting Information) show the 2D graphene-like morphology of the sheets, while their XRD pattern could be indexed to pure rutile SnO_2 with a tetragonal structure (JCPDS no. 88-0287, Figure S2A), which was further verified by the corresponding XPS spectra (Figure S2B–D) and IR spectrum (Figure S3B) that indicated the absence of ethylenediamine on the surfaces. The HRTEM image (Figure 1D) showed the high degree of [001] orientation, which was further confirmed by the corresponding fast Fourier transform image (Figure 1E). The AFM image and corresponding height distribution and height profiles (Figure 1F–H) showed that the overwhelming majority of the sheets possessed an average height of about 0.66 nm, which agreed with the thickness of two unit cells along the [001] direction (Fig-

[*] Dr. Y. F. Sun, F. C. Lei, S. Gao, Prof. B. C. Pan, Prof. Y. Xie
Hefei National Laboratory for Physical Sciences at the Microscale
University of Science & Technology of China
Hefei, Anhui 230026 (P.R. China)
E-mail: yxie@ustc.edu.cn
Dr. J. F. Zhou
Ian Wark Research Institute, University of South Australia
Mawson Lakes, SA 5095 (Australia)

[**] This work was financially supported by the National Basic Research Program of China (2009CB939901), National Nature Science Foundation (11079004, 21201157), Chinese Academy of Science (XDB01020300), Fundamental Research Funds for the Central Universities (WK2310000022), and the Australian Research Council (ARC) Discovery Project (Project ID: DE120101788).

Supporting information (experimental details, sample characterization, calculation details, structural model, formation mechanism, and catalytic activity measurements) for this article is available on the WWW under http://dx.doi.org/10.1002/anie.201305530.

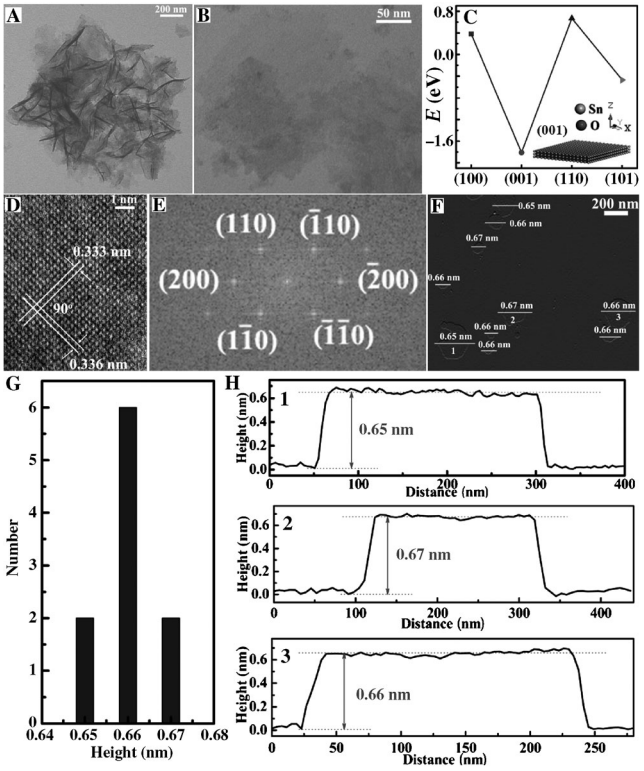

Figure 1. Characterization of SnO_2 sheets. A, B) TEM images, C) calculated adsorption energies (*E*) of ethylenediamine on different facets, D) HRTEM image, and E) corresponding fast Fourier transform, F) AFM image, and corresponding G) height distribution and H) height profiles. The inset in (C) gives the ideal crystal structure; the numbers 1–3 in (F) correspond to the numbers 1–3 in (H).

ure S1). These data offered reliable and direct evidence for the successful synthesis of five-atomic-layer-thick SnO_2 sheets. From our systematic study, we observed that SnO_2 initially nucleated at 180 °C for 30 min (Figure S4 B) and also found that a large amount of SnO particles coexisted in the products when the experiment was performed at 150 °C for 48 h (Figure S4 C–D). In contrast, SnO_2 sheets with a larger thickness of around 1.9 nm were obtained after treatment at 220 °C for 48 h (Figure S5). These results showed that the reaction temperature was crucial for the formation of the 0.66 nm SnO_2 sheets. In addition, the ethylenediamine also played a vital role in the formation of the sheets, as only large and irregular SnO_2 particles were formed in the absence of ethylenediamine (Figure S6). Thus, one can conclude that SnO_2 initially nucleated at 180 °C and simultaneously the ethylenediamine adsorbed on the surface of nuclei to avoid aggregation (Scheme S1). Previous studies showed that the calculated surface energy of tetragonal SnO_2 followed the sequence $(110) < (100) < (101) < (001)$,[15] thus suggesting that the (001) facet with the largest surface energy could possess the highest reactivity compared to other crystal facets. In this case, the ethylenediamine tended to preferentially adsorb on the highly reactive (001) facet, further verified by the calculated adsorption energy in Figure 1 C. This preferential adsorption contributed to lowering the surface energy and hence hindering the crystal growth along the [001] direction, thus resulting in the exposed highly reactive (001) facet. In the absence of ethylenediamine, anisotropic growth along the [001] direction was no longer suppressed, and resulted in the formation of large and irregular SnO_2 particles (Figure S6), thus demonstrating the importance of ethylenediamine. Interestingly, the ethylenediamine could be easily removed from the SnO_2 sheets as it is volatile and soluble in water and alcohol.

As the sheets are five atomic layers (0.66 nm) thick, the surface atoms make up 40% of the total atoms. BET measurements showed that the sheets possess a specific surface area of 173.4 $m^2 g^{-1}$, which is much higher than that of bulk SnO_2 (18.7 $m^2 g^{-1}$; Figure S7). Such a large amount of coordination-unsaturated surface atoms and a much greater surface area may result in unprecedented catalytic properties. To better study the catalytic effect of the SnO_2 sheets on CO oxidation, SnO_2 nanoparticles with an average size of approximately 3 nm and a similar specific surface area of 169.3 $m^2 g^{-1}$ were selected as a reference to compare their catalytic properties.[16] The ignition temperature, corresponding to 10% CO conversion, for the 0.66 nm SnO_2 sheets was 124 °C, which is 79 °C, 146 °C, and 236 °C lower than that of 1.9 nm SnO_2 sheets, SnO_2 nanoparticles, and bulk SnO_2, respectively (Figure 2 A). Furthermore, the 0.66 nm thick SnO_2 sheets have a half-conversion temperature of 165 °C, which is clearly smaller than that for 1.9 nm SnO_2 sheets (239 °C), SnO_2 nanoparticles (327 °C), and bulk SnO_2 (400 °C). In addition, the reaction temperature for full CO conversion over the 0.66 nm SnO_2 sheets was 250 °C, which is significantly lower than that of 1.9 nm SnO_2 sheets (330 °C), SnO_2 nanoparticles (390 °C), and bulk SnO_2 (475 °C). To the best of our knowledge, the reaction temperatures for half and full CO conversion over the 0.66 nm SnO_2 sheets are much lower than all those reported for other forms of parent SnO_2 SnO_2,[6,17] thus strongly highlighting their superior catalytic activity in CO oxidation (Figure 2 C). Moreover, it is well known that the activation energy determines how fast

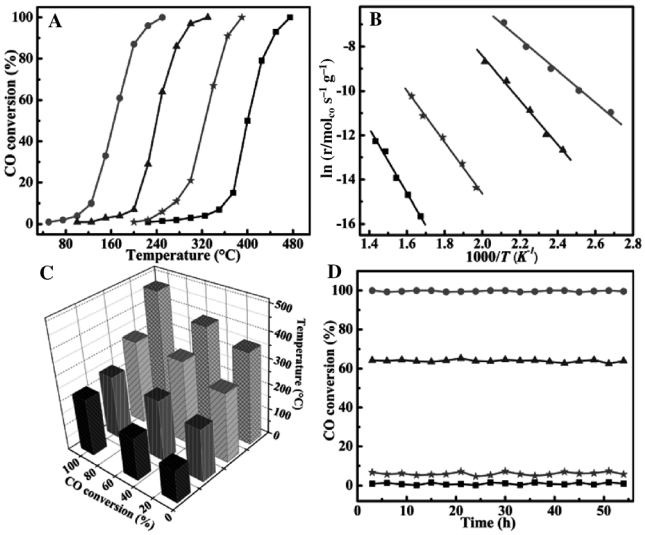

Figure 2. A) Catalytic activity for CO oxidation vs. reaction temperatures, B) corresponding Arrhenius plot, C) 3D histogram of the 10%, 50%, 100% CO conversion vs. reaction temperatures, and D) stability test at 250 °C for 0.66 nm SnO_2 sheets (●), 1.9 nm SnO_2 sheets (▲), SnO_2 nanoparticles (✱), and bulk SnO_2 (■).

a reaction occurs. Figure 2B shows that the 0.66 nm SnO_2 sheets have an apparent activation energy of 59.2 kJ mol^{-1}, which is much smaller than that of 1.9 nm SnO_2 sheets (83.4 kJ mol^{-1}), SnO_2 nanoparticles (101.6 kJ mol^{-1}), and bulk SnO_2 (121.1 kJ mol^{-1}). This result could be attributed to the extremely large fraction of coordination-unsaturated surface atoms, which could serve as the active sites to lower the reaction activation energy. Furthermore, the stability of catalysts is another crucial factor in the evaluation of their catalytic properties. Figure 2D shows that almost no deactivation occurred for the 0.66 nm SnO_2 sheets when the catalytic reaction was conducted at 250 °C for 54 h, thus suggesting excellent structural stability, which was further verified by their TEM images and XRD pattern (Figure S8). In addition, even after the catalytic tests at a higher temperature of 350 °C for 54 h, the 0.66 nm SnO_2 sheets still almost retained their morphologies (Figure S9), further verifying their excellent stability. In contrast, the other three SnO_2 samples, especially the SnO_2 nanoparticles and bulk SnO_2, exhibited obvious deactivation during the catalytic process (Figure 2D), thus indicating their relatively poor stability. Notably, our previous studies demonstrated the presence of obvious structural disorder in ultrathin 2D sheets contributed to their superior structural stability.[7b,11,12] As such, the surface distortion in the 0.66 nm SnO_2 sheets may also account for their excellent cycling stability.

As mentioned above, the 0.66 nm SnO_2 sheets possess an extremely large surface area. Figure 3B shows that the surface Sn atoms have the coordination number 4, which is lower than the value of 6 for the interior Sn atoms, while the surface O atoms have the coordination number 2, which is lower than the value of 3 for the interior O atoms. Notably, the high fraction of surface Sn and O atoms with lower coordination numbers contributed to greatly promoting their catalytic properties. It is widely accepted that the metal oxide catalyzed CO oxidation typically follows the Mars van Krevelen mechanism.[9] Notably, CO oxidation usually occurs at the catalyst surface on account of the lower coordination number and higher catalytic activity of the surface atoms, as further confirmed by DFT calculations. Figure 3A shows that the four-coordinate surface Sn atoms have an adsorption energy (absolute value) of 1.31 eV, which is larger than that of six-coordinate interior Sn atoms, thus suggesting that surface Sn atoms with lower coordination numbers adsorb CO molecules more readily (Figure 3A).[8] In this case, compared to the other three SnO_2 samples, the 0.66 nm thin SnO_2 sheets possessed the highest fraction of surface Sn atoms, which could serve as the catalytically active sites to maximize CO adsorption. The adsorbed CO molecules effectively reacted with the neighboring two-coordinate surface lattice oxygen atoms to form CO_2, which reduced the Sn^{4+} ions to Sn^{2+} ions and simultaneously created an oxygen vacancy in order to maintain charge neutrality (Figure 3C). Note that the coordination-unsaturated lattice oxygen atoms and the low calculated oxygen vacancy formation energy in tetragonal SnO_2 could facilitate the formation of oxygen vacancies on the highly reactive (001) facet,[5] while the created oxygen vacancies exhibited a strong chemical reactivity towards the dissociation of O_2 molecules into highly reactive O atoms, in which one dissociated O atom subsequently replenished the created oxygen vacancies. As such, the significantly large surface area and high fraction of surface atoms mean that the 0.66 nm SnO_2 sheets exhibit remarkably improved catalytic properties for CO oxidation. The 1.9 nm SnO_2 sheets possess a thickness corresponding to six unit cells (Figure S5), only about 15% of the total atoms are exposed on the surface and hence their catalytic properties are much lower than those of the 0.66 nm SnO_2 sheets, which have 40% of their atoms exposed on the surface, thus strongly demonstrating the crucial role of surface atoms in promoting the catalytic oxidation of CO. In addition, the 0.66 nm SnO_2

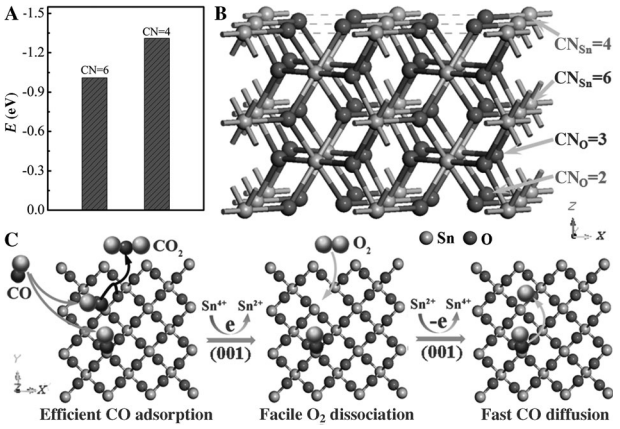

Figure 3. A) Calculated adsorption energies (*E*) for CO molecules on Sn sites with different coordination numbers (CN). B) Crystal structure shows the different CNs for surface and interior atoms. C) Advantages of using the SnO_2 sheets for catalytic CO oxidation: the low-coordinate Sn atom contributes to achieve efficient CO adsorption, the created oxygen vacancy allows for easy O_2 dissociation, and the 2D conducting channel facilitates fast CO diffusion.

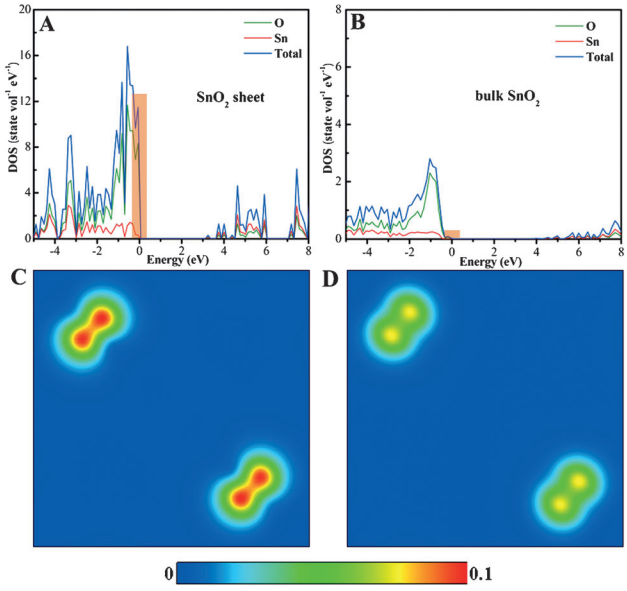

Figure 4. A, B) Calculated density of states (DOS) for the 0.66 nm SnO_2 sheets and bulk SnO_2, insets clearly depict the increased DOS at the valence band edge of the SnO_2 sheets. Charge density contour plots projected along (001) plane for the valence band maximum of C) 0.66 nm SnO_2 sheets and D) bulk SnO_2.

sheets possessed highly improved catalytic properties compared to SnO_2 nanoparticles (Figure 2), despite the similar specific surface area of the two SnO_2 samples. This result implied that the specific surface area was not the decisive factor in determining the catalytic properties, and increased performances could be mainly attributed to their 2D nature and atomic thickness, which facilitate fast electron transport, as was further verified by the calculated DOS in Figure 4. It is well known that the atomic thickness could result in obvious electronic structural variations in the 2D sheets.[7b,11,12] As expected, the 0.66 nm SnO_2 sheets showed significantly increased DOS at the valence band edge with respect to bulk SnO_2 (Figure 4A,B), as was further verified by their calculated charge density contour at the valence band maximum (Figure 4C,D). The enhanced carrier density guaranteed much faster diffusion of a second CO molecule into another dissociated O atom along the 2D conducting channel and sequentially reacted to form CO_2 (Figure 3C), accompanied by the formation of Sn^{4+} ions to end the catalytic cycle. Accordingly, our designed 0.66 nm SnO_2 sheets with an extremely high fraction of low-coordinate surface atoms can fully optimize the elementary adsorption, dissociation, and diffusion steps in the catalytic oxidation of CO.

In conclusion, a model of atomically thin sheets was proposed as a platform to promote catalytic CO oxidation through affording abundant catalytically active sites. Five-atomic-layer-thick 0.66 nm SnO_2 sheets with 40% surface atom occupancy were successfully synthesized in a high-yielding and scalable ethylenediamine-assisted pathway. The high fraction of surface Sn and O atoms with lower coordination numbers than the interior atoms accounted for their improved catalytic properties. The calculated adsorption energies showed that the abundant four-coordinate surface Sn atoms favored CO adsorption, while the adsorbed CO molecule effectively reacted with the neighboring two-coordinate surface lattice oxygen atoms to form CO_2 and simultaneously created an oxygen vacancy, which favored O_2 dissociation into highly reactive oxygen atoms. Moreover, DFT calculations showed that the coordination-unsaturated surface atoms led to the increased density of states at the valence band edge and hence facilitated CO diffusion along the 2D conducting channel to react with the dissociated atomic oxygen atoms. As a result, the 0.66 nm SnO_2 sheets showed remarkably improved CO catalytic performances compared with 1.9 nm SnO_2 sheets, SnO_2 nanoparticles, and bulk SnO_2, with the apparent activation energy lowered to 59.2 kJ mol^{-1} from 121.1 kJ mol^{-1} and the full-conversion temperature reduced by over 200 °C. This work not only provides a facile and scalable strategy for fabricating atomically thin sheets of nonlayered compounds but also proves that the structures are outstanding platforms for fully optimizing the CO oxidation at the atomic level, and thus hold great promise for triggering breakthroughs in low-temperature heterogeneous catalysis.

Received: June 27, 2013
Published online: August 14, 2013

Keywords: atomically thin sheets · carbon monoxide · catalytic oxidation · heterogeneous catalysis · tin dioxide

[1] a) M. Kim, M. Bertram, M. Pollmann, A. V. Oertzen, A. S. Mikhailov, H. H. Rotermund, G. Ertl, *Science* **2001**, *292*, 1357; b) I. X. Green, W. J. Tang, M. Neurock, J. T. Yates, Jr., *Science* **2011**, *333*, 736.

[2] a) A. A. Herzing, C. J. Kiely, A. F. Carley, P. Landon, G. J. Hutchings, *Science* **2008**, *321*, 1331; b) J. L. Gong, R. A. Qjifinni, T. S. Kim, J. M. White, C. B. Mullins, *J. Am. Chem. Soc.* **2006**, *128*, 9012.

[3] a) A. Homés, A. B. Hungría, P. Bera, C. A. López, M. Fernádez-García, L. Barrio, M. Estrella, G. Zhou, J. J. Fonseca, J. C. Hanson, J. A. Rodriguez, *J. Am. Chem. Soc.* **2010**, *132*, 34; b) H. Z. Bao, W. H. Zhang, Q. Hua, Z. Q. Jiang, J. L. Yang, W. X. Huang, *Angew. Chem.* **2011**, *123*, 12502; *Angew. Chem. Int. Ed.* **2011**, *50*, 12294; c) Y. Z. Feng, X. L. Zheng, *Nano Lett.* **2010**, *10*, 4762.

[4] W. M. Haynes, *CRC Handbook of Chemistry and Physics*, CRC, Boca Raton, **2010**, pp. 4–95.

[5] a) C. Kilic, A. Zunger, *Phys. Rev. Lett.* **2002**, *88*, 095501; b) R. Sasikala, N. M. Gupta, S. K. Kulshreshtha, *Catal. Lett.* **2001**, *71*, 69; c) M. Batzill, U. Diebold, *Prog. Surf. Sci.* **2005**, *79*, 47; d) X. R. Zeng, R. B. Zhang, X. L. Xu, X. Wang, *J. Rare Earths* **2012**, *30*, 1013.

[6] Q. R. Zhao, *Trans. Nonferrous Met. Soc. China* **2009**, *19*, 1227.

[7] a) R. F. Service, *Science* **2009**, *324*, 875; b) Y. F. Sun, H. Cheng, S. Gao, Z. H. Sun, Q. H. Liu, Q. Liu, F. C. Lei, T. Yao, J. F. He, S. Q. Wei, Y. Xie, *Angew. Chem.* **2012**, *124*, 8857; *Angew. Chem. Int. Ed.* **2012**, *51*, 8727; c) B. Radisavljevic, A. Radenovic, J. Brivio, V. Giacometti, A. Kis, *Nat. Nanotechnol.* **2011**, *6*, 147; d) Y. W. Zhu, S. Murali, M. D. Stoller, K. J. Ganesh, W. Cai, P. J. Ferreira, A. Pirkle, R. M. Wallace, K. A. Cychosz, M. Thommse, D. Su, E. A. Stach, R. S. Ruoff, *Science* **2011**, *332*, 1537.

[8] a) Q. Fu, W. X. Li, Y. X. Yao, H. Y. Liu, H. Y. Su, D. Ma, X. K. Gu, L. M. Chen, Z. Wang, H. Zhang, B. Wang, X. H. Bao, *Science* **2010**, *328*, 1141; b) J. H. Kwak, J. Z. Hu, D. H. Mei, C. W. Yi, D. H. Kim, C. H. F. Peden, L. F. Allard, J. Szanyi, *Science* **2009**, *325*, 1670.

[9] P. Mars, D. W. Van Krevelen, *Spec. Suppl. Chem. Eng. Sci.* **1954**, *3*, 41.

[10] C. T. Campbell, C. H. F. Peden, *Science* **2005**, *309*, 713.

[11] Y. F. Sun, Z. H. Sun, S. Gao, H. Cheng, Q. H. Liu, J. Y. Piao, T. Yao, C. Z. Wu, S. L. Hu, S. Q. Wei, Y. Xie, *Nat. Commun.* **2012**, *3*, 1057.

[12] Y. F. Sun, H. Cheng, S. Gao, Q. H. Liu, Z. H. Sun, C. Xiao, C. Z. Wu, S. Q. Wei, Y. Xie, *J. Am. Chem. Soc.* **2012**, *134*, 20294.

[13] a) J. S. Chen, X. W. Lou, *Mater. Today* **2012**, *15*, 246; b) S. J. Ding, J. S. Chen, X. W. Lou, *Adv. Funct. Mater.* **2011**, *21*, 4120; c) H. B. Wu, J. S. Chen, X. W. Lou, H. H. Hng, *J. Phys. Chem. C* **2011**, *115*, 24605; d) J. S. Chen, M. F. Ng, H. B. Wu, L. Zhang, X. W. Lou, *CrystEngComm* **2012**, *14*, 5133.

[14] a) S. Ithurria, M. D. Tessier, B. Mahler, R. P. S. M. Lobo, B. Dubertret, A. L. Efros, *Nat. Mater.* **2011**, *10*, 936; b) C. Schliehe, B. H. Juarez, M. Pelletier, S. Jander, D. Greshnykh, M. Nagel, A. Meyer, S. Foerster, A. Kornowski, C. Klinke, H. Weller, *Science* **2010**, *329*, 550.

[15] B. Cheng, J. M. Russell, W. S. Shi, L. Zhang, E. T. Samulski, *J. Am. Chem. Soc.* **2004**, *126*, 5972.

[16] D. L. Chen, L. Gao, *J. Colloid Interface Sci.* **2004**, *279*, 137.

[17] a) S. R. Wang, J. Huang, Y. Q. Zhao, S. P. Wang, X. Y. Wang, T. Y. Zhang, S. H. Wu, S. M. Zhang, W. P. Huang, *J. Mol. Catal. A* **2006**, *259*, 245; b) S. R. Wang, Y. J. Wang, J. Q. Jiang, R. Liu, M. Y. Li, Y. M. Wang, Y. Su, B. L. Zhu, S. M. Zhang, W. P. Huang, S. H. Wu, *Catal. Commun.* **2009**, *10*, 640.

